

Communication

Vortical Differential Scattering of Twisted Light by Dielectric Chiral Particles

Ju Wang, Zhiwei Cui *, Yiyu Shi, Shenyan Guo and Fuping Wu *

School of Physics, Xidian University, Xi'an 710071, China

* Correspondence: zwcui@mail.xidian.edu.cn (Z.C.); fpwu@xidian.edu.cn (F.W.)

Abstract: Twisted light carrying orbital angular momentum inherently possesses a handedness, which would produce chiroptical responses by chiral matter. In this work, a scheme of vortical differential scattering (VDS) was utilized to investigate the chiroptical responses of dielectric chiral particles to the twisted light. The simulation results showed that the dielectric chiral particles have obvious VDS signals under the illumination of twisted light with opposite topological charges. The larger the relative chiral parameter of the particles, the more obvious the VDS signals. The extreme value of the VDS signals can be enhanced by reducing the waist radius of the twisted light or by adopting the circularly polarized twisted light. In addition, non-spherical dielectric chiral particles exhibit more obvious VDS signals compared with spherical ones. These findings are expected to find potential applications in the detection and identification of chiral substances.

Keywords: vortical differential scattering; twisted light; chiral particles

1. Introduction

Chirality, which refers to structures with broken mirror symmetry, arises universally across many different fields [1]. In optics, light with circular polarization has chirality originating from the helical front structure that the electromagnetic field vectors trace out in space when propagating [2]. Each photon of the circularly polarized light carries $\pm\hbar$ spin angular momentum (SAM), with “ \pm ” denoting the left-circular polarization (L-CP) and right-circular polarization (R-CP), respectively, and \hbar being the reduced Planck constant. Light carrying orbital angular momentum (OAM), often referred to as twisted light, also has chirality originating from the helical phase structure [3–9]. Each photon of the twisted light carries $\pm|\ell|\hbar$. OAM, where ℓ is the topological charge and “ \pm ” designates the handedness of the twisted wave front, twisting either to the right or to the left. It has been well recognized that the responses of chiral materials to the light with L-CP and R-CP are different. Such differential responses are well known as the circular dichroism (CD), which has been widely adopted in biology, chemistry, and material science [10]. Recent studies also have shown that chiral materials might respond differently to the handedness of the twisted light carrying OAM [2–8,10–15]. The vortex dichroism (VD) [13], also known as helical dichroism (HD) [14], as well as the circular-vortex dichroism (CVD) [5], vortical differential scattering (VDS) [10], and circular-VDS (CVDS) [2,6] have been introduced to characterize the differential responses of chiral materials to the twisted light with opposite topological charges. Traditionally, chiral materials can be divided into two categories: structural chiral materials and dielectric chiral materials. The chirality of the former is introduced by chiral units whose size is comparable to or larger than the wavelength of interest, while the size of units for the latter is much smaller than the wavelength [16]. Ni et al. theoretically proposed a VDS scheme and experimentally demonstrated that a gigantic VDS of $\sim 120\%$ can be achieved on multiscale particles with chiral structures illuminated by OAM beams [10]. A question naturally arises: do the dielectric chiral particles also have obvious VDS signals to the twisted light carrying OAM? In this paper, we addressed this



Citation: Wang, J.; Cui, Z.; Shi, Y.; Guo, S.; Wu, F. Vortical Differential Scattering of Twisted Light by Dielectric Chiral Particles. *Photonics* **2023**, *10*, 237. <https://doi.org/10.3390/photonics10030237>

Received: 16 January 2023

Revised: 14 February 2023

Accepted: 20 February 2023

Published: 22 February 2023



Copyright: © 2023 by the authors. Licensee MDPI, Basel, Switzerland. This article is an open access article distributed under the terms and conditions of the Creative Commons Attribution (CC BY) license (<https://creativecommons.org/licenses/by/4.0/>).

question by simulating the VDS of various dielectric chiral particles under the illumination of twisted light with Laguerre–Gaussian (LG) mode [17].

The remainder of the paper is organized as follows. In Section 2, we briefly give a description of the theoretical formulae for the problem considered. Section 3 demonstrates the numerical results of this work. Finally, Section 4 concludes the paper.

2. Theoretical Formulae

The LG beams, a typical twisted light, are characterized by two mode numbers, denoted as p and ℓ , respectively, called the radial and azimuthal indices. Here, ℓ is the topological charge as mentioned above. For the simplest form of the LG twisted light with $p = 0$, its angular spectrum amplitude takes the form [18]

$$\tilde{E}(k_x, k_y) = \left(\frac{w_0}{\sqrt{2}}\right)^{|\ell|} [-ik_x + \text{sign}(\ell)k_y]^{|\ell|} \frac{w_0^2}{4\pi} \exp\left[-\frac{w_0^2(k_x^2 + k_y^2)}{4}\right] \quad (1)$$

where $\text{sign}(\ell)$ is the sign function, w_0 is the waist radius of the LG twisted light at $z = 0$, k_x and k_y are the transverse components of the wave vector \mathbf{k} .

Under the paraxial approximation, the vector angular spectrum of the LG twisted light can be written as [19]

$$\tilde{\mathbf{E}}(k_x, k_y) = \left[\alpha\hat{\mathbf{x}} + \beta\hat{\mathbf{y}} - \frac{1}{k}(\alpha k_x + \beta k_y)\hat{\mathbf{z}}\right]\tilde{E}(k_x, k_y) \quad (2)$$

$$\tilde{\mathbf{H}}(k_x, k_y) = \frac{1}{Z} \frac{\mathbf{k} \times \tilde{\mathbf{E}}(k_x, k_y)}{k} \quad (3)$$

where $k = 2\pi/\lambda_0$ and $Z = \sqrt{\mu_0/\epsilon_0}$ are the wave number and impedance in free space, respectively, with λ_0 being the wavelength of the LG twisted light, α and β are the polarization parameters that satisfy the relation $|\alpha|^2 + |\beta|^2 = 1$.

By employing the two-dimensional Fourier transform, the electric and magnetic field vectors of the incident LG twisted light under the paraxial approximation can be expressed as [19]

$$\begin{bmatrix} \mathbf{E}^{inc} \\ \mathbf{H}^{inc} \end{bmatrix} = \exp(ikz) \int_{-\infty}^{\infty} \int_{-\infty}^{\infty} \begin{bmatrix} \tilde{\mathbf{E}}(k_x, k_y) \\ \tilde{\mathbf{H}}(k_x, k_y) \end{bmatrix} \exp\left[i\left(k_x x + k_y y - \frac{k_x^2 + k_y^2}{2k} z\right)\right] dk_x dk_y \quad (4)$$

According to Equations (2) and (3), we can rewrite Equation (4) in the form

$$\mathbf{E}^{inc} = \left[\alpha I_1 \hat{\mathbf{x}} + \beta I_1 \hat{\mathbf{y}} - \frac{1}{k}(\alpha I_2 + \beta I_3)\hat{\mathbf{z}}\right] \exp(ikz) \quad (5)$$

$$\mathbf{H}^{inc} = \frac{1}{Z} \left[-\beta I_1 \hat{\mathbf{x}} + \alpha I_1 \hat{\mathbf{y}} - \frac{1}{k}(\alpha I_3 - \beta I_2)\hat{\mathbf{z}}\right] \exp(ikz) \quad (6)$$

where

$$\begin{bmatrix} I_1 \\ I_2 \\ I_3 \end{bmatrix} = \int_{-\infty}^{+\infty} \int_{-\infty}^{+\infty} \begin{bmatrix} \tilde{E}(k_x, k_y) \\ k_x \tilde{E}(k_x, k_y) \\ k_y \tilde{E}(k_x, k_y) \end{bmatrix} \exp\left[i\left(k_x x + k_y y - \frac{k_x^2 + k_y^2}{2k} z\right)\right] dk_x dk_y \quad (7)$$

Substituting Equation (1) into Equation (7), and performing the integrations, we obtain

$$I_1 = \left(\frac{\sqrt{2}}{w_0}\right)^{|\ell|} \left[\frac{x + i\text{sign}(\ell)y}{1 + iz/z_R}\right]^{|\ell|} \frac{1}{1 + iz/z_R} \exp\left[-\frac{(x^2 + y^2)/w_0^2}{1 + iz/z_R}\right] \quad (8)$$

$$I_2 = -i \left\{ \frac{|\ell| [x - i \text{sign}(\ell)x]}{x^2 + y^2} - \frac{kx}{z_R + iz} \right\} I_1 \tag{9}$$

$$I_3 = -i \left\{ \frac{|\ell| [y + i \text{sign}(\ell)x]}{x^2 + y^2} - \frac{ky}{z_R + iz} \right\} I_1 \tag{10}$$

It is assumed that an LG twisted light is incident on a homogeneous dielectric chiral particle characterized by the relative permittivity, permeability, and chiral parameter $(\epsilon_r, \mu_r, \kappa_r)$, as illustrated in Figure 1a. Such a problem can be solved by employing the method of moments (MoM), based on surface integral equations (SIEs) proposed in [20,21]. Specifically, by introducing equivalent electric and magnetic currents (\mathbf{J}, \mathbf{M}) on the surface S of the particle, as shown in Figure 1b, and applying the equivalence principle to the fields outside and inside the particle, we can obtain a set of SIEs, as follows.

$$\begin{aligned} & \left[Z_0 \mathbf{L}_0(\mathbf{J}) - \mathbf{K}_0(\mathbf{M}) + \frac{1}{2} Z_+ \mathbf{L}_+ \left(\mathbf{J} - \frac{i}{Z} \mathbf{M} \right) - \frac{1}{2} \mathbf{K}_+ (\mathbf{M} + iZ\mathbf{J}) \right. \\ & \left. + \frac{1}{2} Z_- \mathbf{L}_- \left(\mathbf{J} + \frac{i}{Z} \mathbf{M} \right) - \frac{1}{2} \mathbf{K}_- (\mathbf{M} - iZ\mathbf{J}) \right] = -\mathbf{E}^{inc} \Big|_{\tan} \end{aligned} \tag{11}$$

$$\begin{aligned} & \left[\mathbf{K}_0(\mathbf{J}) + \frac{1}{Z_0} \mathbf{L}_0(\mathbf{M}) + \frac{1}{2} \mathbf{K}_+ \left(\mathbf{J} - \frac{i}{Z} \mathbf{M} \right) + \frac{1}{2} \frac{1}{Z_+} \mathbf{L}_+ (\mathbf{M} + iZ\mathbf{J}) \right. \\ & \left. + \frac{1}{2} \mathbf{K}_- \left(\mathbf{J} + \frac{i}{Z} \mathbf{M} \right) + \frac{1}{2} \frac{1}{Z_-} \mathbf{L}_- (\mathbf{M} - iZ\mathbf{J}) \right] = -\mathbf{H}^{inc} \Big|_{\tan} \end{aligned} \tag{12}$$

where the definitions of the integral operators $\mathbf{L}_0, \mathbf{K}_0, \mathbf{L}_\pm,$ and \mathbf{K}_\pm can be found in [20], $Z = \sqrt{\mu_r \mu_0 / \epsilon_r \epsilon_0}, Z_\pm = \sqrt{\mu_\pm / \epsilon_\pm}$ with $\epsilon_\pm = \epsilon_r \epsilon_0 (1 \pm \kappa_r)$ and $\mu_\pm = \mu_r \mu_0 (1 \pm \kappa_r)$.

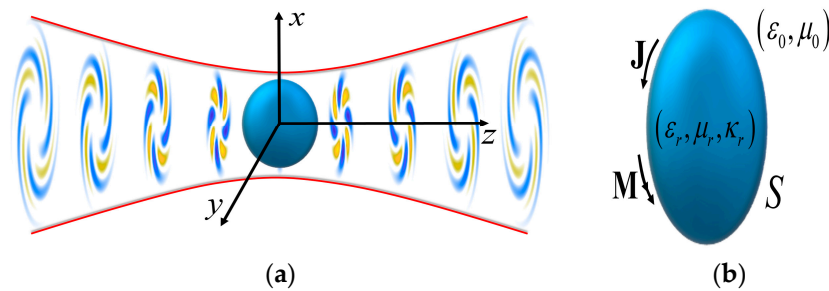


Figure 1. (a) Illustration of a homogeneous dielectric chiral particle illuminated by a twisted light. (b) Schematic of equivalent electric and magnetic currents.

Then, by following the procedure of the well-known MoM [22] based on the Rao, Wilton, and Glisson (RWG) vector basis functions [23], a complete matrix equation system is obtained. After solving this matrix equation, the equivalent sources (\mathbf{J}, \mathbf{M}) on the surface of the particle can be known. Next, we can calculate the scattered field \mathbf{E}_{far}^{sca} in the far-zone according to the following formula:

$$\mathbf{E}_{far}^{sca} = -ik_0 \frac{e^{-ik_0 r}}{4\pi r} \iint_S [Z_0 (\hat{\theta} \hat{\theta} + \hat{\phi} \hat{\phi}) \cdot \mathbf{J}(\mathbf{r}') - (\hat{\theta} \hat{\phi} - \hat{\phi} \hat{\theta}) \cdot \mathbf{M}(\mathbf{r}')] e^{ik_0 \hat{\mathbf{k}} \cdot \mathbf{r}'} dS' \tag{13}$$

in which $\hat{\mathbf{k}} = \sin \theta \cos \phi \hat{\mathbf{x}} + \sin \theta \sin \phi \hat{\mathbf{y}} + \cos \theta \hat{\mathbf{z}}$, with θ and ϕ being the scattering angle and the azimuth angle, respectively.

3. Numerical Results and Discussion

Several numerical simulation results are presented and discussed below. The results are categorized in terms of differential scattering cross section (DSCS) and VDS. The DSCS was defined as

$$\sigma = \lim_{r \rightarrow \infty} 4\pi r^2 \frac{|\mathbf{E}_{far}^{sca}|^2}{|\mathbf{E}_{z=0}^{inc}|^2} \tag{14}$$

and the VDS was defined by a dissymmetry factor as [10]

$$VDS = \frac{I_{+|\ell|} - I_{-|\ell|}}{\left(I_{+|\ell|} + I_{-|\ell|} \right) / 2} \times 100\% \tag{15}$$

where $I_{+|\ell|} = \left| \mathbf{E}_{far}^{sca} \right|_{+|\ell|}^2$ and $I_{-|\ell|} = \left| \mathbf{E}_{far}^{sca} \right|_{-|\ell|}^2$ are the scattering intensities under the illumination of twisted light with topological charges $+|\ell|$ and $-|\ell|$, respectively. In the simulations, the coordinate system of the LG twisted light was coincident with that of the particle. If not otherwise specified, the relative permittivity and permeability of the dielectric chiral particles were chosen as $(\epsilon_r, \mu_r) = (4.0, 1.0)$ and the parameters of the LG twisted light were set as: $\lambda_0 = 632.8$ nm and $(\alpha, \beta) = (1, 0)$, i.e., x -linear polarization (x -LP). For the sake of simplicity, we only calculated the VDS spectra when the topological charge was even. In addition, for the results of the DSCS, we chose the plane with $\phi = 0^\circ$ as the observation plane, and we calculated the backscattered fields for the results of the VDS. Since the validity of the proposed method for analyzing the scattering of LG vortex beams by arbitrarily shaped dielectric chiral particles was demonstrated in our previous work [21], we directly present the numerical results of this work here.

To start, we numerically calculated the DSCSs of a dielectric chiral sphere under the illumination of linearly polarized twisted light with opposite topological charges. The radius and relative chiral parameter of the sphere were $a = 1.0\lambda_0$ and $\kappa_r = 0.5$, respectively, and the waist radius of the incident LG twisted light was $w_0 = 1.0\lambda_0$. Figure 2a shows the angular distributions of the DSCSs for a dielectric chiral sphere illuminated by LG twisted light with opposite topological charges $\ell = \pm 2$. As can be seen, the DSCS for the case of $\ell = +2$ was obviously different from the situation of $\ell = -2$, especially in backscattering. It raises the question of whether such a difference is related to the value of topological charge. To answer this question, we calculated the DSCSs of the aforementioned chiral sphere at scattering angle $\theta = 180^\circ$ illuminated by LG twisted light with topological charge $|\ell|$ from 0 to 20, as shown in Figure 2b, where the results were smoothed. Again, we observed an obvious difference between the DSCSs for the cases of $+\ell$ and $-\ell$. It was observed that the difference varied with the topological charge. These results demonstrate that the responses of dielectric chiral particles to the twisted light with opposite topological charges are different. As mentioned earlier, such differential responses can be characterized by using the VDS.

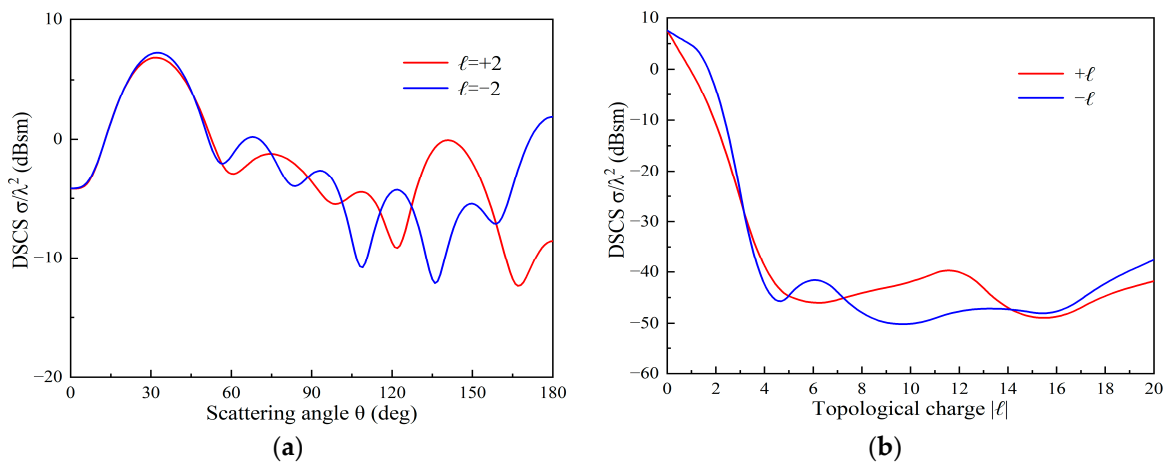


Figure 2. (a) Angular distributions of the DSCSs for a dielectric chiral sphere illuminated by LG twisted light with opposite topological charges $\ell = \pm 2$. (b) DSCSs at scattering angle $\theta = 180^\circ$ for a dielectric chiral sphere illuminated by LG twisted light with topological charge $|\ell|$ from 0 to 20.

Regarding the VDS spectra of dielectric chiral particles under the illumination of LG twisted light, we focused on the effects of the relative chiral parameter, size, and shape of the particle, as well as the beam waist and polarization state of the incident twisted light on the VDS spectra. Figure 3 shows the VDS spectra of dielectric chiral spheres with different relative chiral parameters. The radius of the spheres was $a = 1.0\lambda_0$ and the waist radius of the incident LG twisted light was $w_0 = 2.0\lambda_0$. The intrinsic chiral asymmetry of the particle was found to have a significant influence on the VDS spectra. For all three cases considered, the VDS spectra exhibited an obvious valley at $|\ell| = 2$. Moreover, with the increase in the relative chiral parameter, the valley value decreased, i.e., its absolute value increased. Note that the greater the absolute value, the more obvious the VDS signal.

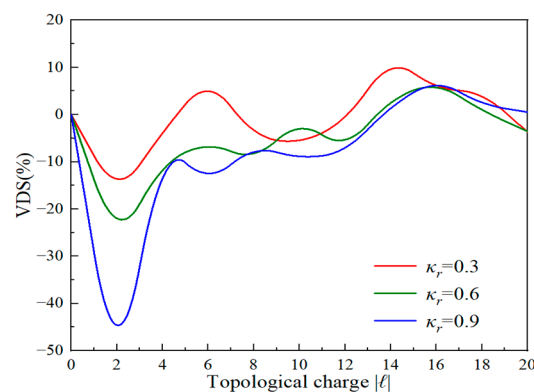


Figure 3. VDS spectra of dielectric chiral spheres with different relative chiral parameters.

Figure 4 shows the VDS spectra of dielectric chiral spheres with different radii for a given incident LG twisted light. The relative chiral parameter of the spheres was assumed to be $\kappa_r = 0.9$ and the waist radius of the incident LG twisted light was set as $w_0 = 1.0\lambda_0$. It can be observed that when the radius of the sphere was just equal to the waist radius of the LG twisted light, i.e., $a = w_0 = 1.0\lambda_0$, the VDS signal was much less than that of other cases and the VDS spectrum did not exhibit an obvious peak or valley. When $a = 0.5\lambda_0 (< w_0)$, the VDS spectrum exhibited an obvious valley at $|\ell| = 2$. Whereas when $a = 1.5\lambda_0 (> w_0)$, the VDS spectrum exhibited an obvious peak at $|\ell| = 18$ and the maximum VDS value of $\sim 140\%$ was obtained. The above results indicate that the relationship between the size of the particle and the waist radius of the twisted light has a significant influence on the VDS. To verify this conclusion, we further examined the VDS of a dielectric chiral sphere induced by an LG twisted light with different waist radii, as exhibited in Figure 5. The radius and the relative chiral parameter of the sphere were set as $a = 1.0\lambda_0$ and $\kappa_r = 0.9$, respectively. We found that the VDS spectrum exhibited an obvious peak at $|\ell| = 12$ when $w_0 = 0.5\lambda_0 (< a)$, whereas it exhibited an obvious valley at $|\ell| = 2$ when $w_0 = 1.5\lambda_0 (> a)$. The above results indicate that the VDS signal can be enhanced by reducing the waist radius of the incident LG twisted light.

As mentioned earlier, circularly polarized light has chirality, and linearly polarized twisted light carrying OAM also has chirality. Another interesting question in this paper arose: how was the VDS affected by the polarization state of the twisted light? Figure 6 shows the VDS of a dielectric chiral sphere illuminated by an LG twisted light with different polarization states, where x -LP, L-CP, and R-CP corresponded to the LG twisted light with x -linear polarization, left-circular polarization, and right-circular polarization, respectively. The radius and the relative chiral parameter of the sphere were $a = 1.0\lambda_0$ and $\kappa_r = 0.9$, respectively, and the waist radius of the incident LG twisted light was $w_0 = 2.0\lambda_0$. From Figure 6, it was found that the state of polarization had a significant effect on the VDS. The VDS value for the case of linearly polarized twisted light was less than that for the cases of circularly polarized twisted light, indicating that circularly polarized twisted light can enhance the VDS signal. A further observation we made was that the VDS spectra for the cases of twisted light with x -LP and R-CP exhibited a valley, whereas the VDS spectrum

exhibited a peak for the case of twisted light with L-CP. In addition, the absolute value of the peak signal for twisted light with L-CP was less than that of the valley signal for twisted light with R-CP.

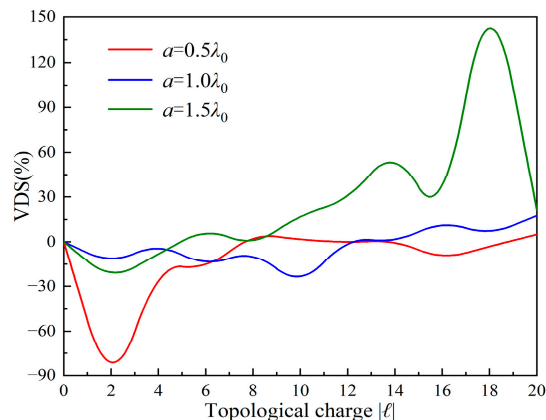


Figure 4. VDS spectra of dielectric chiral spheres with different radii for a given incident LG twisted light with waist radius $w_0 = 1.0\lambda_0$.

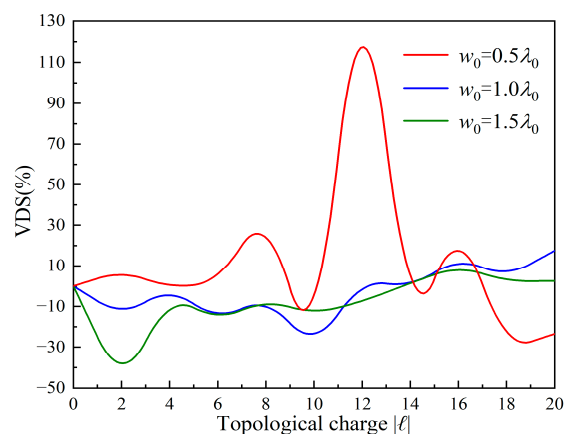


Figure 5. VDS spectra of a dielectric chiral sphere induced by an LG twisted light with different waist radii.

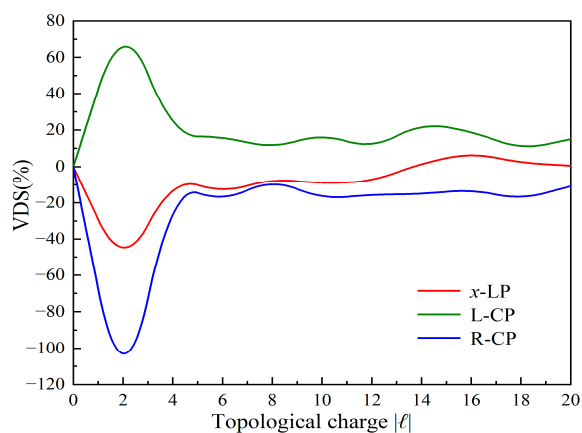


Figure 6. VDS spectra of a dielectric chiral sphere induced by LG twisted light with different polarization states.

Finally, Figure 7 depicts the comparison of the VDS spectra from dielectric chiral sphere, spheroid, and cylinder under the illumination of a twisted light with $w_0 = 2.0\lambda_0$.

The radii of the sphere and cylinder as well as the semi-minor axis of the spheroid were assumed to be the same and were set as $1.0\lambda_0$. The semi-major axis of the spheroid was $2.0\lambda_0$ and the height of cylinder was $4.0\lambda_0$. The relative chiral parameter of all these three particles was chosen as $\kappa_r = 0.9$. It can be seen from Figure 7 that the VDS spectra of these three types of particles with the same projection area perpendicular to the beam propagation direction exhibited an obvious valley at $|\ell| = 2$. Notably, non-spherical dielectric chiral particles had a more obvious VDS signal. Moreover, the extreme value of the VDS signal for the spheroid was larger than that for the cylinder.

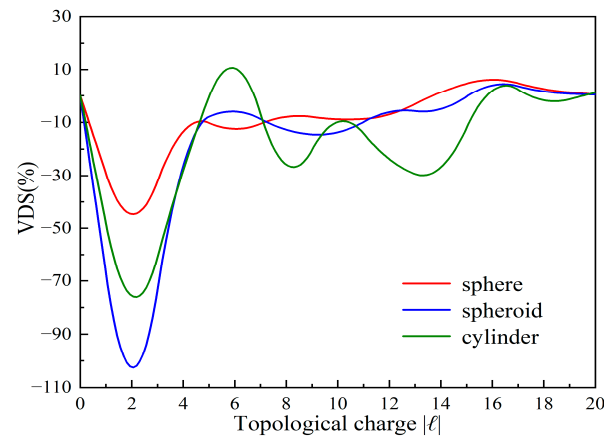


Figure 7. Comparison of the VDS spectra from dielectric chiral sphere, spheroid, and cylinder.

4. Conclusions

In conclusion, we investigated numerically the chiroptical responses of dielectric chiral particles to the LG twisted light with opposite handedness. A scheme of VDS was introduced to characterize such chiroptical responses. The electric and magnetic field vectors of the LG twisted light under the paraxial approximation were derived based on vector angular spectrum representation. The MoM based on SIEs was utilized to solve the scattering problems involving dielectric chiral particles with arbitrary shapes. Some numerical simulations were performed and discussed. The results showed that the responses of dielectric chiral particles to the LG twisted light with opposite topological charges were different. The VDS spectrum of a dielectric chiral particle induced by twisted light strongly depends on the relative chiral parameter, size, and shape of the particle, as well as the beam waist and polarization state of the incident twisted light. Increasing the relative chiral parameter of the particle caused the VDS signal to become increasingly clear. The relationship between the size of the chiral particle and the waist radius of the twisted light had a significant influence on the VDS spectrum, whose extreme value could be enhanced by reducing the waist radius of the incident LG twisted light. Circularly polarized twisted light also could enhance the VDS signal. In addition, compared with spherical chiral particles, non-spherical chiral particles had more obvious VDS signals. These results are expected to advance our understanding of the interactions between LG twisted light with chiral matter and benefit the applications of chiral detection and identification.

Author Contributions: Conceptualization, J.W. and Z.C.; methodology, S.G. and F.W.; software, Y.S.; validation, Y.S.; investigation, J.W. and Z.C.; writing—original draft preparation, J.W. and Z.C.; writing—review and editing, F.W.; supervision, Z.C.; funding acquisition, F.W. All authors have read and agreed to the published version of the manuscript.

Funding: This research was funded by the 111 Project, grant number B17035; Natural Science Basic Research Program of Shaanxi, grant number 2023-JC-YB-536; Natural Science Foundation of Guangdong Province, grant number 2022A1515011138.

Institutional Review Board Statement: Not applicable.

Informed Consent Statement: Not applicable.

Data Availability Statement: Not applicable.

Acknowledgments: The authors would like to thank the editor and anonymous reviewers who handled our paper.

Conflicts of Interest: The authors declare no conflict of interest.

References

1. Mun, J.; Kim, M.; Yang, Y.; Badloe, T.; Ni, J.C.; Chen, Y.; Qiu, C.W.; Rho, J. Electromagnetic chirality: From fundamentals to nontraditional chiroptical phenomena. *Light Sci. Appl.* **2020**, *9*, 139. [\[CrossRef\]](#)
2. Forbes, K.A.; Andrews, D.L. Enhanced optical activity using the orbital angular momentum of structured light. *Phys. Rev. Res.* **2019**, *1*, 033080. [\[CrossRef\]](#)
3. Araoka, F.; Verbiest, T.; Clays, K.; Persoons, A. Interactions of twisted light with chiral molecules: An experimental investigation. *Phys. Rev. A* **2005**, *71*, 055401. [\[CrossRef\]](#)
4. Brullot, W.; Vanbel, M.K.; Swusten, T.; Verbiest, T. Resolving enantiomers using the optical angular momentum of twisted light. *Sci. Adv.* **2016**, *2*, e1501349. [\[CrossRef\]](#)
5. Forbes, K.A.; Andrews, D.L. Optical orbital angular momentum: Twisted light and chirality. *Opt. Lett.* **2018**, *43*, 435–438. [\[CrossRef\]](#)
6. Forbes, K.A. Raman optical activity using twisted photons. *Phys. Rev. Lett.* **2019**, *122*, 103201. [\[CrossRef\]](#)
7. Forbes, K.A. Nonlinear chiral molecular photonics using twisted light: Hyper-Rayleigh and hyper-Raman optical activity. *J. Opt.* **2020**, *22*, 095401. [\[CrossRef\]](#)
8. Forbes, K.A.; Andrews, D.L. Orbital angular momentum of twisted light: Chirality and optical activity. *J. Phys. Photonics* **2021**, *3*, 022007. [\[CrossRef\]](#)
9. Wang, B.; Tanksalvala, M.; Zhang, Z.; Esashi, Y.; Jenkins, N.W.; Murnane, M.M.; Kapteyn, H.C.; Liao, C.T. Coherent Fourier scatterometry using orbital angular momentum beams for defect detection. *Opt. Express* **2021**, *29*, 3342–3358. [\[CrossRef\]](#)
10. Ni, J.C.; Liu, S.L.; Wu, D.; Lao, Z.X.; Wang, Z.Y.; Huang, K.; Ji, S.Y.; Li, J.W.; Huang, Z.X.; Xiong, Q.H.; et al. Gigantic vortical differential scattering as a monochromatic probe for multiscale chiral structures. *Proc. Natl. Acad. Sci. USA* **2020**, *118*, e2020055118. [\[CrossRef\]](#)
11. Ye, L.; Rouxel, J.R.; Asban, S.; Rösner, B.; Mukamel, S. Probing molecular chirality by orbital angular momentum carrying X-ray pulses. *J. Chem. Theory Comput.* **2019**, *15*, 4180–4186. [\[CrossRef\]](#)
12. Wozniak, P.; Leon, I.D.; Hoflich, K.; Leuchs, G.; Banzer, P. Interaction of light carrying orbital angular momentum with a chiral dipolar scatterer. *Optica* **2019**, *6*, 961–965. [\[CrossRef\]](#)
13. Forbes, K.A.; Garth, A.J. Optical vortex dichroism in chiral particles. *Phys. Rev. A* **2021**, *103*, 053515. [\[CrossRef\]](#)
14. Ni, J.C.; Liu, S.L.; Hu, G.W.; Hu, Y.L.; Lao, Z.X.; Li, J.W.; Zhang, Q.; Wu, D.; Dong, S.H.; Chu, J.R.; et al. Giant helical dichroism of single chiral nanostructures with photonic orbital angular momentum. *ACS Nano* **2021**, *15*, 2893–2900. [\[CrossRef\]](#)
15. Sakamoto, M.; Uemura, N.; Saito, R.; Shimobayashi, H.; Yoshida, Y.; Mino, T.; Omatsu, T. Chirogenesis and amplification of molecular Chirality using optical vortices. *Angew. Chem. Int. Ed.* **2021**, *60*, 12819–12823. [\[CrossRef\]](#)
16. Zhao, R.; Li, J.Q.; Zhang, Q.; Liu, X.G.; Zhang, Y.J. Behavior of SPPs in chiral-graphene-chiral structure. *Opt. Lett.* **2021**, *46*, 1975–1978. [\[CrossRef\]](#)
17. Allen, L.; Beijersbergen, M.W.; Spreeuw, R.J.C.; Woerdman, J.P. Orbital angular momentum of light and the transformation of Laguerre-Gaussian laser modes. *Phys. Rev. A* **1992**, *45*, 8185–8189. [\[CrossRef\]](#)
18. Wu, F.P.; Cui, Z.W.; Guo, S.Y.; Ma, W.Q.; Wang, J. Chirality of optical vortex beams reflected from an air-chiral medium interface. *Opt. Express* **2022**, *30*, 21687–21697. [\[CrossRef\]](#)
19. Song, P.; Cui, Z.W.; Hui, Y.F.; Zhao, W.J.; Wang, J.J.; Han, Y.P. Explicit analytical expressions for the electromagnetic field components of typical structured light beams. *J. Quant. Spectrosc. Radiat. Transf.* **2020**, *241*, 106715. [\[CrossRef\]](#)
20. Worasawate, D.; Mautz, J.R.; Arvas, E. Electromagnetic scattering from an arbitrarily shaped three-dimensional homogeneous chiral body. *IEEE Trans. Antennas. Propag.* **2003**, *51*, 1077–1084. [\[CrossRef\]](#)
21. Cui, Z.W.; Guo, S.Y.; Wang, J.; Wu, F.P.; Han, Y.P. Light scattering of Laguerre-Gaussian vortex beams by arbitrarily shaped chiral particles. *J. Opt. Soc. Am. A* **2021**, *38*, 1214–1223. [\[CrossRef\]](#) [\[PubMed\]](#)
22. Harrington, R.F. *Field Computation by Moment Methods*; Macmillan: New York, NY, USA, 1968.
23. Rao, S.M.; Wilton, D.R.; Glisson, A.W. Electromagnetic scattering by surfaces of arbitrary shape. *IEEE Trans. Antennas. Propag.* **1982**, *30*, 409–418. [\[CrossRef\]](#)

Disclaimer/Publisher's Note: The statements, opinions and data contained in all publications are solely those of the individual author(s) and contributor(s) and not of MDPI and/or the editor(s). MDPI and/or the editor(s) disclaim responsibility for any injury to people or property resulting from any ideas, methods, instructions or products referred to in the content.